

DESIGN OF AN EXPERIMENTAL SET-UP TO DETERMINE THE INFLUENCE OF CORROSION ON HEAT TRANSFER

W. Faes^{1,2*}, S. Lecompte¹, J. Van Bael², R. Salenbien², M. Billiet¹ and M. De Paepe¹

¹ Department of Flow, Heat and Combustion Mechanics, Ghent University, Sint-Pietersnieuwstraat 41, 9000 Ghent, Belgium

² VITO, Boeretang 200, 2400 Mol, Belgium

*Author for correspondence

E-mail: Willem.Faes@UGent.be

ABSTRACT

In the exploitation of geothermal energy, heat exchangers are essential to distribute heat to energy conversion systems (e.g. organic Rankine cycles) or district heating networks. The geothermal brine found in Belgium however has a high temperature and a high salinity which makes it extremely corrosive. In such environments, the classic solution is to construct a heat exchanger with a highly corrosion resistant metal such as titanium or nickel. However, since these metals are very expensive, alternatives are investigated. One such alternative is using heat exchangers made of less corrosion resistant materials, but where detailed information about the corrosion process is available. This information is then used during design and for predictive maintenance. An experimental set-up to determine the corrosion rate and the influence of corrosion on the heat transfer is designed.

INTRODUCTION

In the context of Europe's energy and climate targets, a strong drive exists towards the use of renewable energy. Geothermal energy, being the thermal energy generated and stored in the Earth, is an interesting resource. The heat can be used in district heating networks or electricity can be generated with systems like an organic Rankine cycle (ORC). The composition of the pumped geothermal water can vary a lot depending on the drilled earth layer. In the campina of Limburg and Antwerp for instance, the carboniferous limestone layer contains 3 to 4 times more salt compared to sea water. Moreover, the production temperature of the brine can be up to 130°C. Hence, the geothermal water is very corrosive to conventional materials which are used for heat exchangers and piping. Special materials, such as titanium, need to be used. Due to the high salt content and the high temperature, materials like titanium and nickel with are required. This gives problems regarding machinability and weldability and the heat exchanger investment cost increases significantly. Compared to a stainless steel heat exchanger, the investment cost is about 8 times higher. The evaporator of a geothermal ORC project with a water cooled condenser accounts about 10% of the total ORC [1]. If the evaporator cost increases with a factor 8, then the ORC cost increases with 70%. This has a strong impact on the profitability of the geothermal project.

An alternative is to use cheaper metals, like e.g. stainless steel. These materials are less corrosion resistant, so details on the corrosion rate in the geothermal

environment and on the influence of the corrosion on the heat exchanger performance are required in the design phase of the heat exchanger.

Other fields where corrosion often causes problems in heat transfer equipment are oil refining plants, chemical industries, electric power plants, food and liquor processing, paper manufacture, refrigeration and air conditioning [2].

Corrosion in heat exchangers can take many forms. The risk of several types of corrosion can be greatly reduced by a careful design. Galvanic corrosion can for example be avoided by using the same metal for different parts or by electrically insulating dissimilar metals. Crevice corrosion is a type of corrosion taking place in small, narrow areas and is caused by the differential oxygen concentration that exists in these places. In shell-and-tube heat exchangers, this can e.g. be between the tubes and the tubesheets. Welding these gaps can solve this problem. However, welds are a dangerous area for intergranular corrosion (localized corrosion attack at the grain boundaries [3]), so they should be executed by skilled technicians. Cold formed plates or bends in tubes often have residual stresses, making them prone to stress corrosion. A proper heat treatment can in these cases have beneficial effects. Finally, it is advised to avoid stagnant or low-velocity areas in the heat exchanger, because this is where pitting corrosion typically occurs. [4]

Most studies investigating corrosion are performed because of economic reasons [2]. Already in the design phase, the possibility of corrosion can increase the cost of the heat exchanger. More expensive materials may be chosen or the heat exchanger may be overdesigned. Increased maintenance needs cause higher costs during the operation of the heat exchanger. Failure of the heat exchanger can finally create long down-times of production and loss of products (possibly with an expensive impact on the environment)

In addition to costs originating from the material side, corrosion can also cause a decrease in thermohydraulic performance. Although one might expect that a decrease in wall thickness of the heat transfer surface would cause an increase in the heat transfer rate, a decrease in efficiency is often observed. This is caused by a phenomenon called corrosion fouling where the corrosion products do not detach from the surface or are deposited on the surface downstream in the heat exchanger [5]. These corrosion products then form an additional resistance to the heat transfer. Another thermal resistance influenced by corrosion is the film convection resistance. Corrosion increases surface roughness, creating more turbulence and thus

increasing the heat transfer [6]. However this higher turbulence will reflect in a higher required pumping power. This is similar to the roughness controlled phase typically occurring with precipitation fouling (crystallization of solids from solutions on the heat transfer surface [7]), as seen in Figure 1 [8].

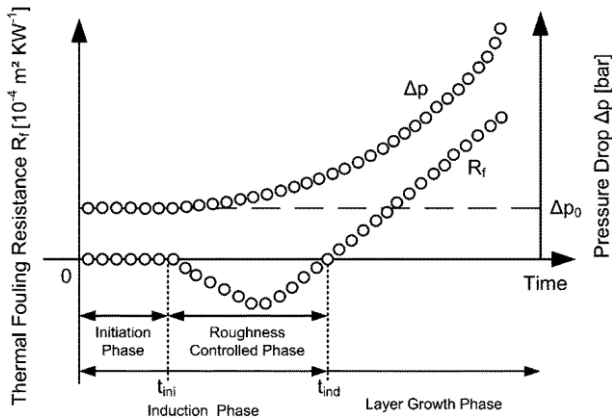


Figure 1 Evolution of thermal fouling resistance and pressure drop for precipitation fouling [8]

To be able to quantify the corrosion rate inside a tube with flowing geothermal brine and to determine the influence of the corrosion (and corrosion fouling) on the heat transfer performance, an experimental set-up will be build. Knudsen [9] already discussed several techniques to measure fouling (not necessarily corrosion fouling) of heat transfer surfaces. The author classified different set-ups according to geometry, method of heating (or cooling) and method of monitoring the deposit. The possibilities mentioned by the author are listed in Table 1.

Table 1 Possible set-up designs to measure fouling on heat transfer surfaces [9]

Geometry	Heating	Deposit monitoring
Inside tube	Sensible fluid heating	Visually
Annulus	Condensing vapour	Direct weighing
Sphere	Electrical resistance	Microscopically
Outside of U-tube	Indirect electrically	Pressure drop
Metallic strip	Thermoelectric	Thermally
Plate		Radioactively
Wire		Electrolytically
Wire coil		Chemically
Shell		
Helix		

Of the many possible combinations, several apparatus are described by Knudsen [9], e.g. the one shown in Figure 2. This set-up exists of a double-pipe heat exchanger, where the fouling fluid can flow in either the annulus or the tube. This fluid is heated or cooled by a clean fluid flowing in the other passage with either co-current or countercurrent flow. By comparing the outlet temperatures in fouled conditions

with the ones in clean conditions, a fouling factor can be calculated.

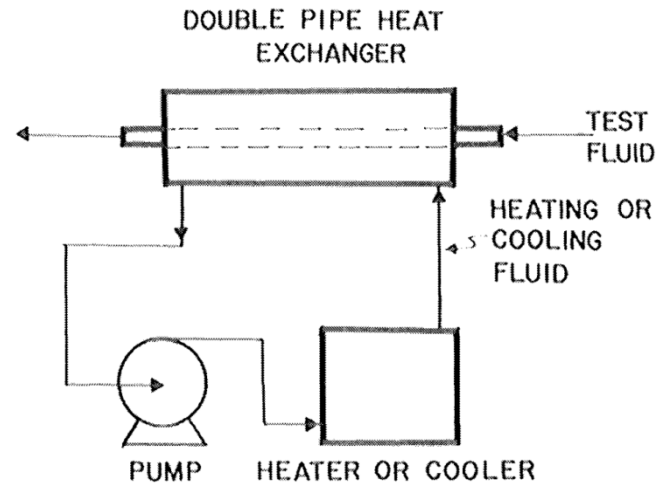


Figure 2 Double pipe heat exchanger set-up to measure fouling resistances [9]

In this paper, an adaptation of the apparatus described above is discussed. The difference is that the process inside the tube is not a deposition of material on the wall but rather a gradual reduction of the wall thickness, caused by corrosion, combined with possibly some corrosion fouling.

SET-UP DESIGN

Lay-out

Similar to the set-up described by Knudsen, the current design is a double-pipe heat exchanger. In a straight tube with flow, the corrosion process will be faster than in static conditions because of erosion. The behaviour of (erosion-) corrosion in bends is different from that in straight tubes, therefore a U-bend is integrated, dividing the double-pipe heat exchanger in two parts. This bend will be insulated to limit the heat losses to the environment. In this device, the aggressive brine flows inside the tube and clean water in counterflow in the annulus. This way, only the inner surface of the small pipe will suffer corrosion while its outer surface and the outer pipe remain in clean conditions. Both fluids will be circulating in a separate loop.

Since the fluid in a geothermal plant is at high temperatures, the brine will be heated by an external heater and cooled in the heat exchanger by the cooling water. This cooling water will be cooled by an external cooling device. In both loops a pump will be present to circulate the fluid in the tubes. A schematic overview of the set-up is given in Figure 3.

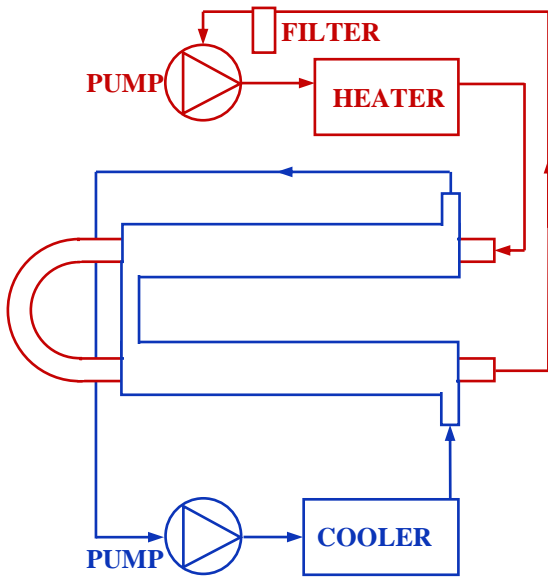


Figure 3 Schematic lay-out of experimental set-up

Thermohydraulic Design

Although the production temperature of the geothermal well is around 130°C, an inlet temperature of the experiment of 80°C was chosen. This was done because flow sensors for such corrosive applications at high temperatures are either unavailable or extremely expensive. The inlet temperature of the cooling water, provided by a chiller, was set at 10°C. Since one of the goals of the experiment is to determine the influence of fluid flow on the corrosion process, the velocity of the brine should be high enough. A velocity of 3 m/s was chosen.

To limit the heating and cooling power, it was decided to keep the heat transferred in the heat exchanger under 6 kW. An iterative design procedure led to a loop where the brine outlet temperature is 62°C and the inner diameter of the tube is 6 mm. The resulting power is 5.8 kW. To avoid premature failure of the set-up due to high localized corrosion rates, a tube wall thickness of 3 mm was chosen. This means that the tube has an outer diameter of 12 mm.

For the outer tube, an inner diameter of 20 mm and a flow rate of 0.24 kg/s (1.2 m/s) were chosen. Based on the heat balance, this results in a cooling water outlet temperature of 15.8°C.

In the calculation of the required length of the heat exchanger, the properties of clean water were used for the cooling water side. Since the brine closely resembles seawater with very high salinity, the thermodynamic properties (density, specific heat, thermal conductivity and viscosity) are calculated for seawater. The correlations for these properties in function of temperature and salinity are given in a review by Sharqawy *et al.* [10]. For the density, the correlation given by Isdale and Morris [11] was used. The specific heat is calculated with the correlation given by Jamieson *et al.* [12]. The correlation given by Jamieson and Tudhope [13] was used to determine the thermal conductivity and the viscosity was calculated with the correlation given by Isdale *et al.* [14].

In these correlations a temperature of 80°C and a salinity of 160 g/kg were used. The resulting values for the brine and the cooling water are given in Table 2.

Table 2 Thermophysical properties of cooling water and brine

	Cooling water	Brine
Density (kg/m ³)	995.7	1 090
Specific heat (J/kg K)	4 178	3 509
Therm. Cond. (W/m K)	0.611	0.659
Viscosity (N s/m ²)	0.00080	0.00054
Prandtl Number (-)	5.46	2.88

The Reynolds numbers inside the tube and the annulus are respectively $3.6 \cdot 10^4$ and $1.2 \cdot 10^4$, indicating that the flow is turbulent. To calculate the Nusselt numbers, the correlations shown in Eq. (1) and Eq. (2) are used [15], valid for $10^4 < Re < 5 \cdot 10^6$ and $0.5 < Pr < 200$.

$$f = (1.58 \cdot \ln(Re_b) - 3.28)^{-2} \quad (1)$$

$$Nu_b = \frac{(f/2) \cdot Re_b \cdot Pr_b}{1.07 + 12.7 \cdot (f/2)^{1/2} \cdot (Pr_b^{1/2} - 1)} \quad (2)$$

The result is an overall heat transfer coefficient calculated for the cooling water side in clean conditions of $U_o = 953.3 \text{ W/m}^2 \text{ K}$, which results, with a logarithmic mean temperature difference of $\Delta T_{\text{lmtd}} = 57.9^\circ\text{C}$, in a total required heat exchanger length of $L = 2.81 \text{ m}$.

Material and Part Selection

The goal of the experiment is to determine the influence of the fluid flow on the corrosion process and the effect of this corrosion on the heat transfer performance. The corroding tube should be constructed of a metal that is not completely corrosion resistant, but the corrosion should not be too fast either. A material that gradually thins, at e.g. one millimetre per two months, without suffering localized corrosion would be ideal. Such a material will be selected by performing static corrosion tests prior to the construction of the set-up.

The inner surface of the small tube is however the only surface that should corrode in the experiment, meaning that all other components in the brine loop should be resistant to this aggressive environment. Therefore, all wetted surfaces should be made of either expensive alloys (like e.g. titanium) or polymers.

For connecting the heat exchanger with the pump and the heater, PTFE hoses will be used. Such hoses are available for temperatures up to 200°C.

Pumping the geothermal fluid will be done with a diaphragm pump. This is a positive displacement pump where no pistons or impellers are in contact with the fluid. Only a flexible diaphragm that is driven by a piston is used to move the fluid. Diaphragm pumps moulded out of PTFE with PTFE diaphragms are available for the required flow rates and up to 100°C. The pump is air-driven and a

pulsation damper is required to assure a smooth flow. Before the pump, a filter will be installed to the iron oxide from entering the pump.

Electric immersion heaters are commonly made of metals that are not corrosion resistant in the brine. An alternative are inline heaters used to heat aggressive liquids used in e.g. the semiconductor industry. Such heaters exist in 6 kW versions (close to the 5.8 kW mentioned earlier) and typically made of fluoropolymers like PTFE or PFA.

On the cooling water side, more standard parts can be used, since this water is at lower temperatures and does not contain corrosive ions. This means that no PTFE is required for connecting the heat exchanger with the chiller.

Different chillers exist able of cooling continuously with a sufficient cooling power. These chillers typically come with a build-in circulation pump.

Monitoring

To measure the changes in performance of the heat exchanger, several sensors will be installed on the set-up.

Three ultrasonic thickness sensors will be installed on the outside small tube: one at the inlet, one at the outlet and one on the bend. Ultrasonic thickness sensors calculate the wall thickness by measuring the time an ultrasonic wave needs to travel from the outer surface to the inner surface and back. There are sensors available that can measure both the remaining thickness of the tube and the thickness of the fouling oxide layer. The two sensors on the straight parts allow determining the influence of the fluid flow on the corrosion rate at two different temperatures by comparing the obtained results with results from prior performed static tests. In the bend, the corrosion rate is expected to be higher than in the straight parts due to the effect of erosion-corrosion. This will be measured by the third thickness sensor.

To calculate the heat transfer coefficients, temperature measurements will be performed at the inlet, middle and outlet of the hot and cold circuit. These will be performed PT100 temperature sensors.

Also necessary for the calculation of the heat transfer coefficient are the flow rates. On the cold side, these can be measured easily with e.g. turbine flow sensors, vortex flow sensors or magnetic inductive flow sensors. On the brine side, standard flow sensors would suffer corrosion. Therefore, there will be opted for a PTFE coated magnetic flow sensor.

Finally, two pressure sensors, one at the inlet and one at the outlet of the brine circuit, will be used to determine if the flow passage increases because of the corrosion or decreases by corrosion-fouling.

Where all the sensors will be placed on the set-up can be seen on Figure 4.

EXPECTED RESULTS

When the set-up is built and the monitoring tools are ready, the brine will be circulated in the heat exchanger for an extended period until the thickness of the inner tube has reduced by e.g. 50%. At this point, the influence on the heat transfer performance should be sufficiently large and the tube will still be strong enough. During this extended

period, temperatures, pressures, thicknesses and flow rates will continuously be measured and stored.

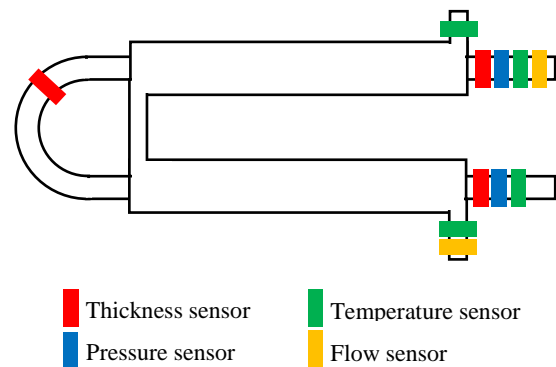


Figure 4 Position of the sensors on the set-up

A first result of the experiment is the corrosion rate as a function of time. It is expected that the initial corrosion rate will be high, but decreases when a stable oxide film is formed. Prior to the experiment, static corrosion tests will have been performed at the same temperature. A comparison of the results will give an idea of the influence of the erosion effect caused by the fluid flowing at 3 m/s. In the bends, the erosion-corrosion is anticipated to be higher since the wall shear stresses are higher.

The influence of the corrosion on the heat transfer is more difficult to predict. On one hand, the corrosion reduces the wall thickness, decreasing its thermal resistance, but on the other hand, iron oxide deposits can form an insulating layer. Measurements with the ultrasonic thickness sensors, able to give both remaining wall thickness and oxide layer thickness should indicate which process is prevalent. Also the possibility of detecting this with pressure drop measurements will be tested.

It is expected that, because of the high flow rate at the brine side, the corrosion will have a bigger influence than the corrosion fouling. If only corrosion would be present and no iron oxides deposit on the surface, the outlet temperatures and the heat transfer coefficient can be calculated for constant inlet and outlet temperatures and constant mass flow rates. The resulting outlet temperatures for a reduction in wall thickness up to 50% (or 1.5 mm corroded) are shown in Figure 5, together with the measurement uncertainty (the error analysis is described later). It can be seen that the brine outlet temperatures would decrease, while the cooling water outlet temperatures increase. Figure 6 shows the evolution of the overall heat transfer coefficient. Also here, the measurement uncertainty is shown. With only corrosion, the overall heat transfer coefficient would increase from 953 W/m² K to 1304 W/m² K, or an increase of 36.8%.

After the experiment, the tube will be extracted from the double pipe heat exchanger and samples will be longitudinally cut in half. A visual inspection will indicate whether only uniform corrosion is present or if signs of localized forms of corrosion (like pitting corrosion) are also

visible. An analysis of the corrosion products will reveal more details on the nature of the corrosion process.

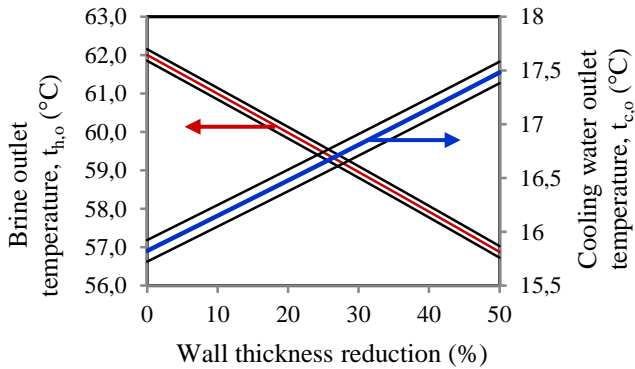


Figure 5 Calculated outlet temperatures for a wall thickness reduction up to 50% with constant inlet temperatures and mass flow rates

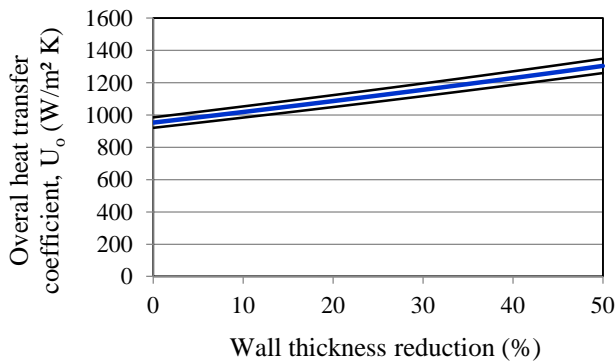


Figure 6 Calculated overall heat transfer coefficient for a wall thickness reduction up to 50% with constant inlet temperatures and mass flow rates

The results of the experiment will then be combined into a model to predict what performance can be expected of a heat exchanger used in the geothermal application after a certain period. This will allow to design a heat exchanger with a certain corrosion allowance and to predict when maintenance is required. In this way, expensive costs of unexpected replacements of a failed heat exchanger can be avoided.

Error Analysis

To determine whether the obtained results are relevant with respect to the measurement errors, an error analysis on the calculation of the overall heat transfer coefficient and on the corrosion rate were made. A relative error on the overall heat transfer coefficient of maximally $\pm 3.4\%$ was found, while with a 10% reduction in wall thickness, the heat transfer coefficient, calculated like in Figure 6, already increases with 6.4%. The relative error on the corrosion rate is decreasing with reducing wall thickness. When 0.2 mm of the tube wall has corroded, the error found on the corrosion rate is already smaller than $\pm 5\%$. More details on the error analysis can be found in the appendix at the end of the paper.

FUTURE RESEARCH POTENTIAL

When the experiment is finished and has proven to be able to monitor corrosion rates and its influence on the heat transfer, some extensions of the set-up can be made.

Firstly, more experiments on the same set-up will be made. The corrosion rate will be measured at different temperatures and at different flow rates. Also other steel alloys will be tested.

Next, corrosion monitoring tools, other than those based on wall thickness or pressure drop monitoring will be tested and evaluated. Two relatively straightforward examples are corrosion coupons and electrical resistance measurements. A corrosion coupon is a small specimen exposed to the flow and removed after a certain period for weight loss measurements, while with electrical resistance measurements, the resistance of a corroding wire placed in the flow is monitored. The more the wire has corroded, the higher its resistance will be. Other types of monitoring techniques are a variety of electrochemical methods. These can give information on the instantaneous corrosion rate, but are less easy to interpret. (Roberge, 2000)

Finally, the protection of the tube against corrosion can be tested. By placing a sacrificial anode in the stream, the corrosion of the pipe might be reduced. Also the application of an impressed current to decrease the corrosion rate is an option.

CONCLUSIONS

In this paper, the design of a set-up that will be used to observe the behaviour of a heat exchanger in a corrosive (geothermal) environment is described.

Thermal calculations for a double-pipe heat exchanger with a bend in the middle resulted in a total length of 2.81 m. The inlet temperatures of the brine and the cooling water are respectively 80°C and 10°C. In the heat exchanger, 5.8 kW will be transferred. In the inner tube, the heated brine will flow at 3 m/s, while the cooling water will be in the annulus. Flow rates, temperatures, pressures and wall thicknesses will be monitored continuously.

The brine will flow for an extended period, while temperatures, pressures, wall thicknesses and flow rates will be monitored. This will allow calculating the evolution of the overall heat transfer coefficient and the corrosion rate. The error on the heat transfer measurement is calculated to be $\pm 3.4\%$, which should be sufficiently accurate to detect the effect of the corrosion on the heat transfer.

It is expected that the uniform corrosion rate under flow will be higher than under static conditions. The influence of the corrosion on the heat transfer will be depending on whether the corrosion products stay in solution or are deposited on the heat transfer surface. If the reducing of the wall thickness would be the only effect present, without corrosion fouling, a wall thickness reduction of 10% is calculated to give an increase in heat transfer of 6.4%.

ACKNOWLEDGEMENTS

This work was done with the support of the EU, ERDF, Flanders Innovation & Entrepreneurship and the Province of Limburg.

NOMENCLATURE

f	Friction factor, dimensionless
Nu	Nusselt number, dimensionless
Pr	Prandtl number, dimensionless
Re	Reynolds number, dimensionless
T	Temperature, °C
U	Overall heat transfer coefficient,

Subscript

b	Bulk conditions
lmtd	Logarithmic mean temperature difference
o	Outer

APPENDIX

Error analysis

The uncertainties on the density and specific heat of the brine, calculated with the correlations of Isdale and Morris [11] and Jamieson *et al.* [12] are $\pm 0.1\%$ and $\pm 0.28\%$ respectively. The temperature sensors can be calibrated to an accuracy of $\pm 0.1^\circ\text{C}$, while the flow sensors are calibrated in the factory to an accuracy of $\pm 0.35\%$. The other values, necessary to calculate the overall heat transfer coefficient are assumed known. The error on the wall thickness measurements, necessary for the calculation of the corrosion rate is ± 0.01 mm. For the error propagation, Eq. (3) was used.

$$q = q(x, y) \Rightarrow \sigma_q = \sqrt{\left(\frac{\delta q}{\delta x} \sigma_x\right)^2 + \left(\frac{\delta q}{\delta y} \sigma_y\right)^2} \quad (3)$$

REFERENCES

- [1] Walraven, D., Laenen, B., and D'haeseleer, W., 2015, Minimizing the levelized cost of electricity production from low-temperature geothermal heat sources with ORCs: Water or air cooled?, *Applied Energy*, Vol. 142, pp. 144-153.
- [2] Kuppan, T., 2000, *Heat exchanger design handbook*, CRC Press, Chapter 12, pp. 579-580.
- [3] Roberge, P. R., 2000, *Handbook of corrosion engineering*. McGraw-Hill, Chapter 6, pp. 417-428.
- [4] Shah, R. K. and Sekulic, D. P., 2003, *Fundamentals of heat exchanger design*, John Wiley & Sons.
- [5] Somerscales, E. F., 1997, Fundamentals of corrosion fouling, *Experimental thermal and fluid science*, Vol. 14, pp. 335-355.
- [6] Ross, T. K., 1967, Corrosion and Heat Transfer review, *British Corrosion Journal*, Vol. 2, pp. 131-142.
- [7] Melo, L. F., Bott, T. R. and Bernardo, C. A., 1988, *Fouling Science and Technology*.
- [8] Schoenitz, M., Grundemann, L., Augustin, W., and Scholl, S., 2015, Fouling in microstructured devices: a review, *Chemical Communications*, Vol. 51, pp. 8213-8228.
- [9] Knudsen, J. G., 1981, Apparatus and techniques for measurement of fouling of heat transfer surfaces, *Fouling of heat transfer equipment*, 57-81.
- [10] Sharqawy, M. H., Lienhard, J. H., and Zubair, S. M., 2010, Thermophysical properties of seawater: a review of existing correlations and data, *Desalination and Water Treatment*, Vol. 16, pp. 354-380.
- [11] Isdale, J. D., Morris, R., 1972, Physical properties of sea water solutions: density, *Desalination*, Vol. 10, pp. 329-339.
- [12] Jamieson, D. T., Tudhope, J. S., Morris, R., Cartwright, G., 1969, Physical properties of sea water solutions: heat capacity, *Desalination*, Vol. 7, pp. 23-30.
- [13] Jamieson, D. T., Tudhope, J.S., Physical properties of sea water solutions – Thermal conductivity, *Desalination*, Vol.8, pp. 393-401.
- [14] Isdale, J. D., Spence, C. M., Tudhope, J. S., Physical properties of sea water solutions: viscosity, *Desalination*, Vol. 10, pp. 319-328.
- [15] Petukhov, B. S., 1970, Heat transfer and friction in turbulent pipe flow with variable physical properties, *Advances in heat transfer*, Vol. 6, pp. 503-564.